Formation of metal-ceramic interfaces : a surface science approach

M. Gautier, J. Duraud

Classification
Physics Abstracts
73.60D — 68.22 — 68.55 — 82.80P

Formation of metal-ceramic interfaces : a surface science approach

M. Gautier ([1]) and J. P. Duraud ([2])

([1]) Direction des Sciences de la Matière, Service de Recherche sur les Surfaces et l'Irradiation de la Matière, CEA, Bât. 462, CEN Saclay, 91191 Gif-sur-Yvette Cedex, France
([2]) Laboratoire Pierre Süe, CEA/CNRS, CE Saclay, 91191 Gif-sur-Yvette Cedex, France

(*Received 28 February 1994, accepted 20 June 1994*)

Résumé. — Les interfaces métal-céramique interviennent dans de nombreuses technologies, où l'on recherche des propriétés électriques, optiques, magnétiques ou mécaniques particulières. Ces propriétés dépendent des caractéristiques des interfaces, comme leur structure atomique et leur composition, ainsi que la nature des liaisons interfaciales. L'étude des étapes initiales de la formation de l'interface métal-céramique, par condensation de la vapeur métallique sur la surface céramique préparée et caractérisée *in-situ*, permet d'accéder à ces caractéristiques. Les méthodes d'étude des surfaces qui reposent sur la détection des électrons émis sous un faisceau de photons ou d'électrons, peuvent alors être utilisées pour obtenir des informations sur l'interface, à condition que la couche métallique déposée ait une épaisseur inférieure au libre parcours moyen des électrons détectés. Au moyen de quelques exemples, nous montrons comment il est possible de suivre, au fur et à mesure que l'interface se forme : le mode de croissance du film métallique sur la surface céramique, la structure atomique de l'interface (ordre à longue et courte distance), l'établissement des liaisons chimiques, la composition de l'interface, et la formation éventuelle d'un composé d'interface.

Abstract. — Metal-ceramic interfaces are involved in a great number of technologies, where specific electrical, optical, magnetic or mechanical properties are required. These properties often depend on the characteristics of the interfaces, such as their atomic structure and composition, as well as the nature of the interfacial bonds. Such relevant characteristics can be obtained by studying the initial stages of the metal-ceramic interface formation, the metallic deposit being condensed from a vapor phase, onto the *in situ* prepared and well characterized ceramic surface. The usual surface science methods relying on the detection of the electrons emitted under an electron or photon beam can then be used *in situ*, and information on the interface can be obtained, while it is being formed, provided that the deposited metallic layer is thinner than the escape depth of the detected electrons. Through some examples, we show how it is possible to follow, when the interface is being formed : the growth mode of the metallic film onto the ceramic surface, the atomic structure at the interface (long range and short range order), the chemical bond formation, the composition of the interface, and the possible formation of an interfacial new compound.

1. Introduction.

Metal-ceramic interfaces are of great importance in various fields such as : heterogeneous catalysis, cermets, microelectronics, wetting of ceramics by liquid metals, thermomechanics

(metal-ceramic joining), magnetic components based on metallic multilayers, and metallic coatings for optical devices.

Whatever may be the application, the required property (optical, mechanical, electrical..) depends on the interface characteristics.

The relevant characteristics of a given ceramic-metal interface are twofold :

1.1 THE ATOMIC STRUCTURE AND THE COMPOSITION OF THE INTERFACE. — The nature of the interface can be diffuse or abrupt. The rôle of interdiffusion processes at the interface is of great importance and should be elucidated. In the case of important lattice parameter misfit between the ceramic and the metal, interface dislocations may appear, which can affect the quality of the interface.

Moreover, the possible formation of an interface compound has to be studied.

1.2 THE NATURE OF THE INTERFACE BONDS. — Different kinds of bonds can exist at the interface : either chemical bonds (metal-metal or metal-oxygen) or van der Waals. As an example, figure 1 illustrates the Al_2O_3 model surface used by McDonald and Eberhart [1]. For the adsorbed metal atoms, two types of sites were taken into account : metal atoms directly above locations that would extend the cation lattice were regarded as being chemically bonded while the others were considered to be attached only by van der Waals forces. In both cases, only metal-oxygen bonds were taken into account. Such a model considers neither the possible chemical reactions at the interface, or the contribution to the adhesion energy of the metal-cation bonds, which can not be neglected, as was shown for the Pt-Al_2O_3 interface for instance [2]. Some recent works dealing with the nature of the interfacial bonds, and aimed at evaluating the different contributions of these bonds to the adhesion energy have been developed and are reviewed in reference [3].

In order to get insight into the interface characteristics, two approaches can be used.

The first one consists in studying an interface already built : *a buried interface*. As far as the atomic structure of the interface is concerned, high resolution transmission microscopy has proved to be a powerful method [4].

Another promising technique is the grazing incidence X-ray diffraction [5], which has been until now widely used for semiconductor interfaces. A very recent work has been carried out on the Nb (111)-Al_2O_3 (0001) interface, and an atomistic model was proposed, which contains a soliton-type deformed lattice due to the presence of misfit dislocations in the interface [6].

As concerns the composition at the interface, Rutherford backscattering spectroscopy (RBS) can be used mainly for deep interfaces. For instance, the interface reactions between titanium thin films and a $(1\bar{1}02)$ sapphire surface have been studied [7]. A 200 to 400 nm thick Ti film

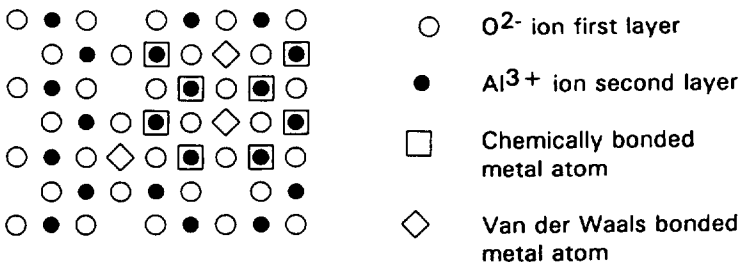

Fig. 1. — Al_2O_3 model surface used by McDonald and Eberhart model (taken from [2]).

was RF sputtered onto a monocristalline $(1\bar{1}02)$ Al_2O_3 surface, the temperature of the substrate being controlled and ranging from 525 and 660 °C. A further annealing of the interface led to the formation of an intermetallic compound Ti_3Al, the thickness of which could be derived from the RBS data, and the diffusion controlled growth evidenced. One advantage of this method is that it is non destructive, but its poor depth resolution (a few tens Å) is a limiting factor. For this reason the methods relying on the sputtering of the material until the interface is reached, are sometimes preferred : either secondary ion mass spectroscopy (SIMS) or surface analysis methods such as Auger electron (AES) or X-ray photoelectron (XPS) spectroscopies, coupled with ion bombardment so as to obtain concentration profiles at the interface. The depth resolution is better (a few Å), but one has to face the differential sputtering, which can produce changes in the interface composition, if great care is not taken [8].

Another possibility consists in studying the *initial stages of the formation of a model metal-ceramic interface*, in an ultra-high vacuum multichamber apparatus, allowing :

- the *in situ* preparation of the ceramic surface, and the characterization of the surface composition, electronic and crystallographic structures ;
- the condensation of the metallic deposit, from a vapor phase, onto the as-prepared ceramic surface.

The usual surface science method relying on the detection of the electrons emitted under an electron or photon beam can then be used *in situ*, and information on the interface can be derived, provided that the deposited metallic layer is thinner than the escape depth of the detected electrons.

This approach, where measurements are performed simultaneously when the interface is being formed *in situ via* successive metal deposition cycles, enables one to investigate the dynamic processes of interface formation. With the use of UHV systems, the influence of contaminants at the surface can be eliminated, or at least, controlled, which allows to study the direct interaction between the relevant components [9].

It is then possible to follow, when the interface is being formed :

i) the growth mode of the metallic film onto the ceramic surface ;

ii) the atomic structure at the interface, from the point of view of the long range order but also of the short range order ;

iii) the chemical bond formation ;

iv) the composition of the interface, and the possible formation of an interfacial new compound.

2. Growth mode.

The different steps of the formation of thin films of metals on ceramic oxide surfaces have been extensively reviewed in [10].

The initial step in the formation of a metallic film is the impingement of metal atoms on the substrate. After landing, the metal atoms can immediately be reflected from the substrate surface. They can also adsorb and either stick permanently to the substrate, or reevaporate within a finite time. In the two latter cases, the atoms are accomodated, that means that they give part of their kinetic energy to the substrate.

Condensation can occur only if the flux of adsorbed atoms is larger than the flux of reevaporated atoms, i.e. if the supersaturation ratio is larger than 1. When this ratio reaches 1, the vapor-substrate system is in equilibrium. The mean residence time of an adsorbed atom before reevaporation is finite and can be written as : $\tau_a = (1/\nu) . \exp(\Delta G_{des}/kT)$, where

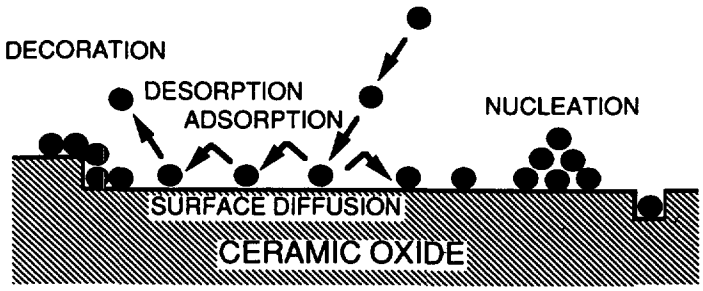

Fig. 2. — Main steps in the first stages of the formation of metal thin films on an oxide ceramic surface (taken from [10]).

ΔG_{des} is the free activation energy for the desorption process. Then condensation of a permanent deposit may not be possible even if the substrate temperature is so low that the evaporation rate, S of the film material in the bulk at that temperature is negligible ($S \gg 1$). However, condensation of a permanent deposit on the substrate does occur at sufficiently high impingement rates, because the interactions between adsorbed single atoms cannot be neglected. Due to the diffusion processes, which are highly temperature dependent, adsorbed atoms can migrate over the surface, giving rise to collisions with other atoms, and clusters can form. This is the nucleation stage. Figure 2 represents schematically the first stages of nucleation.

Most nucleation theories postulate an equilibrium or steady state to exist between the adsorbed monomers, which diffuse on the substrate surface for a time τ_a, constantly colliding with themselves and other clusters of various sizes. Once a cluster has reached a given critical size, it will, on the average, no longer dissociate into monomers, but will grow to form a stable condensate [11].

On an ideally perfect surface, without defects, random nucleation can occur. However, if defects are present at the surface, such as steps for instance, they can act as preferential nucleation sites. Indeed preferential deposition of metals at steps or extended defects is used to

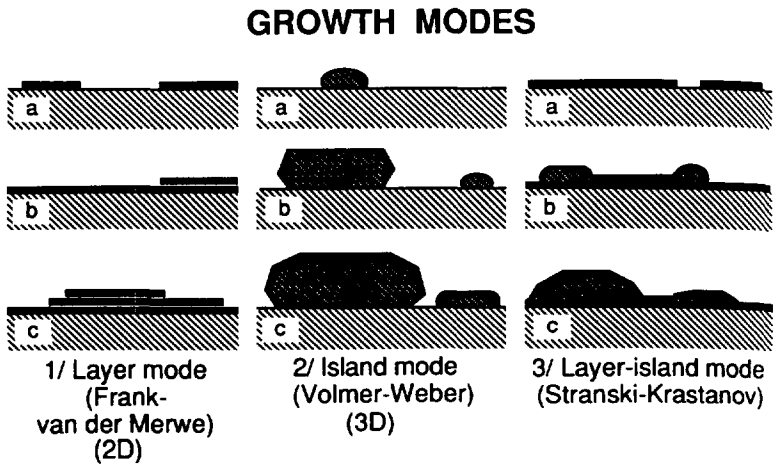

Fig. 3. — The three main growth modes of thin metallic films on oxides (from [10]).

reveal the surface irregularities (decoration) [12]. The nuclei can be either two-dimensional, or tri-dimensional, depending on the growth mode. In the case of non reactive metal-substrate systems, three main growth modes are distinguished (Fig. 3) :

i) the layer-by-layer mode or Franck-van der Merwe mode (two-dimensional or 2D mode) corresponds to a strong metal-ceramic adhesion strength compared with cohesion between metallic atoms ;

ii) the island or Volmer-Weber mode (three-dimensional or 3D mode) occurs when the cohesion energy of the metal is strong compared to the adhesion energy between particle and substrate ;

iii) the layer-island mode or Stranski-Krastanov mode corresponds to the formation of 3D nuclei onto a metallic film grown layer by layer.

This describes a model situation, where the metal vapor is condensed onto a substrate at low temperature T_s, under ultra-high-vacuum, with a very low oxygen partial pressure p_{O_2}, as in a MBE (Molecular Beam Epitaxy) experiment. If the temperature T_s or the oxygen partial pressure p_{O_2} are increased, an interfacial compound may form : interdiffusion and alloying then play an important role.

Then, in a given experiment, the relevant growth parameters are :

- *the substrate temperature*, which will influence all diffusion and possible interdiffusion processes, as well as the possibility of epitaxy (when a critical temperature for epitaxy exists, above which epitaxy is no longer possible). It will also play a rôle on the defect density at the surface,
- *the impinging vapor flux*, which determines the nucleation rate ;
- *the ambient pressure*, and particularly the oxygen partial pressure p_{O_2} ;
- *the substrate conditioning :* the crystallographic structure is a determining parameter for epitaxy, the presence of defects may influence the nucleation mode and the quality of the interface, and the substrate surface composition can change the nature of the chemical interfacial bonds.

It should be mentioned that such a study of the growth mode has a more general scope : indeed the problem of determining the shape of a solid particle in equilibrium with the substrate is analogous to that of describing the shape of a liquid droplet under similar conditions. This offers the opportunity to obtain information on the wetting properties of the metal-ceramic system. This aspect was first argued in [13], and further documented in [10, 14]. Strictly speaking, for the analogy to be valid, the shape of the particle grown from the vapor phase onto the substrate should be studied with the substrate at the same temperature than in the wetting experiment, generally the temperature of the liquid metal. Indeed the growth mode depends on the substrate temperature, even for metals on metals [15, 16].

The droplet shape is characterized by a contact angle θ, which is defined as the angle between the surface of the droplet at the point of contact with the surface-droplet interface [17]. For crystalline solids, the surface energy γ is anisotropic and the contact angle can no longer uniquely determine the particle shape. However the shape theory of Winterbottom classifies the substrate-particle configurations into four types, according to the degree of wetting, as displayed in figure 4 (reproduced from [14]). The liquid droplet shapes are shown on the right hand side for comparison.

The predicted shape of a single crystal particle expected to be observed in an experiment appears as a solid line. A measure of the degree of wetting is provided by the quantity $\gamma_{sp} - \gamma_{sv}$, where s denotes the substrate, p the particle and v the vapor. Two different heights can be measured : the height h from the substrate surface to the maximum diameter parallel to the substrate, which is proportional to $\gamma_{sp} - \gamma_{sv}$, and the height H from the maximum diameter

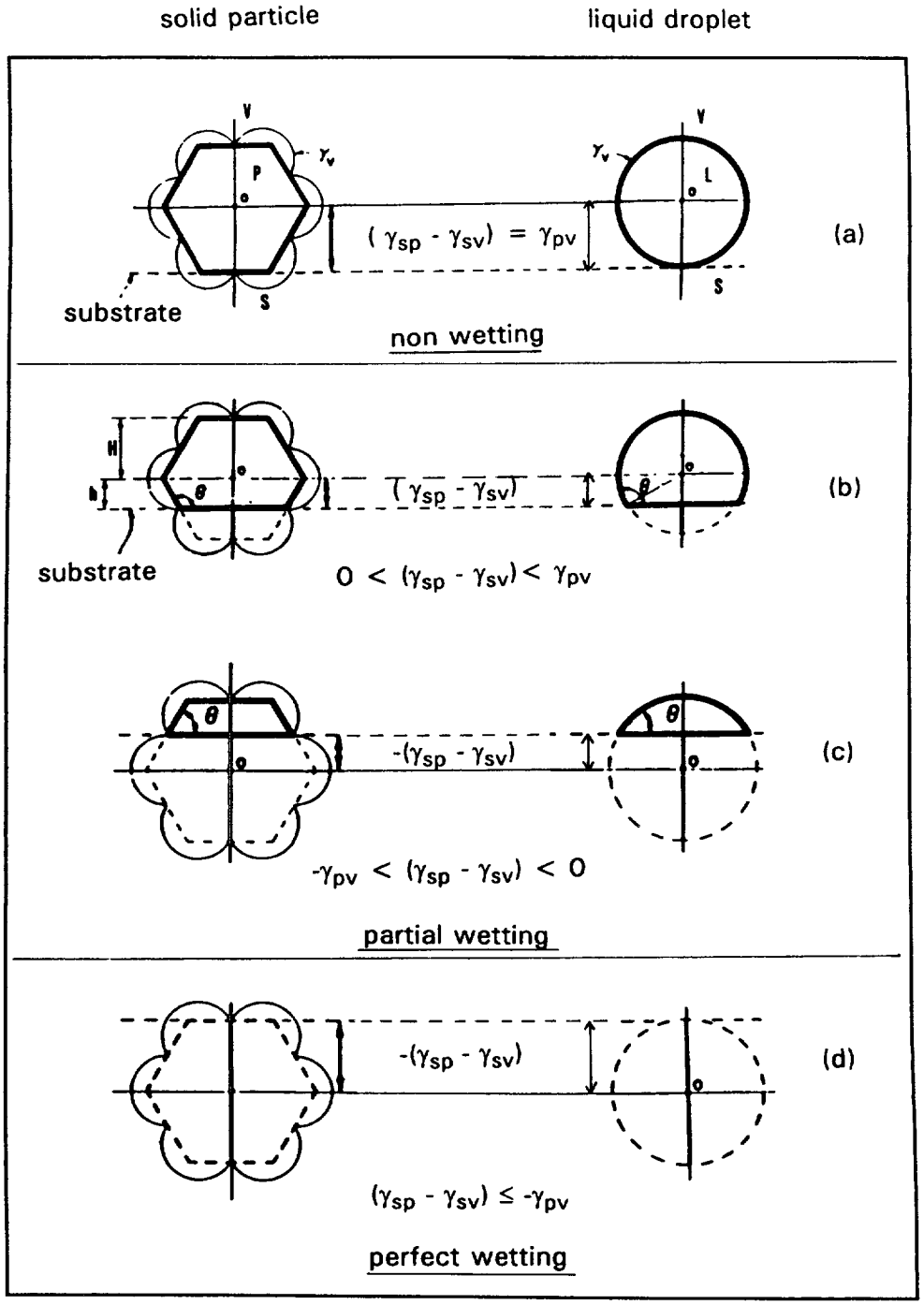

Fig. 4. — The general surface energy plots and corresponding equilibrium shape (strong line) for a two-dimensional solid and liquid, for different wetting configurations : non-wetting (a), partial wetting (b) and (c), complete wetting (d) (from [14]).

parallel to the substrate to the apex of the particle, which is proportional to γ_{pv}. Then the work of adhesion, defined as the energy required to separate the metal from the substrate can be derived as : $E_{ad} = \gamma_{pv}(1 - h/H)$. This method was applied to obtain values of E_{ad} for the interfaces Cu/Al_2O_3 [14], Pd/Al_2O_3 [18].

In the case of the formation of a metallic film onto an oxide ceramic surface, the examples of layer by layer growth are very scarce, and the 3D growth mode are the more frequent (Stranski-Krastanov and Volmer-Weber) [10].

The characterization of the growth modes is one of the many prominent uses of electron spectroscopies. A typical experiment involves a measurement of the intensity of a characteristic Auger electron line from the substrate, or from the deposit, as a function of overlayer thickness. In the layer by layer mode, the characteristic shape of these curves is a series of straight lines with breaks at coverages corresponding to an integral number of monolayers. The different slopes (positive for the deposit, negative for the substrate) are due to attenuation of the Auger signal across the different deposited layers. For the substrate, the envelope of points at integral coverage follows an exponential decay $\exp(-nd/\lambda)$, where d is the thickness of a metal monolayer and λ the inelastic mean free path of the substrate Auger electrons across the deposit. When the number of deposited layers is large, the signal from the substrate approaches 0, whereas that of the deposit approaches that of the bulk signal.

In the layer-islanding mode (Stranski-Krastanov), the curves exhibit one (or several) linear parts in coïncidence with those of the layer by layer mode, corresponding to the completion of one (or several) layers. In the second stage of growth (islanding), like in the Volmer-Weber mode, the deposited material forms islands of unspecified dimensions and the actual attenuation depends on the fraction of covered surface. Figure 5, taken from reference [19], shows typical extinction curves for the Auger signal of the substrate. In these examples, the inelastic mean free path is taken as 2 monolayers, and for the cases involving islanding, it is assumed that 50 % of the surface is covered. It must be noted that in the two latter modes, the Auger yield from the substrate does not theoretically approach the zero yield associated with

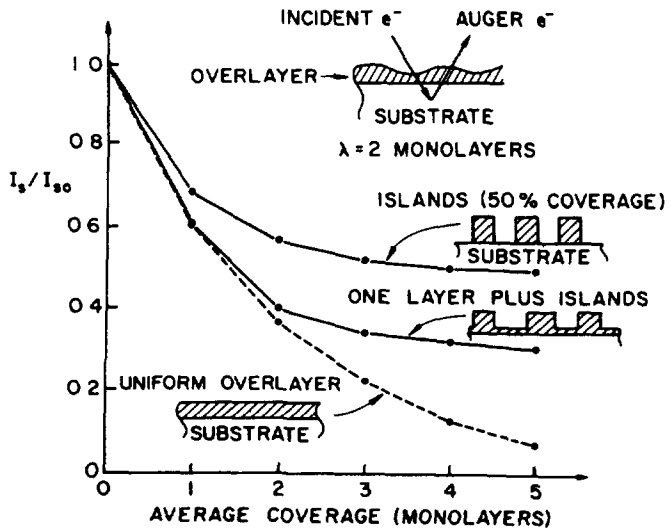

Fig. 5. — Extinction curves for the Auger signal characteristic of the substrate, as a function of average coverage of the metallic overlayer : the three different modes, layer by layer (Franck-van der Merwe), layer-islanding (Stranski-Krastanov), and islanding (Volmer-Weber), are represented (from [19]).

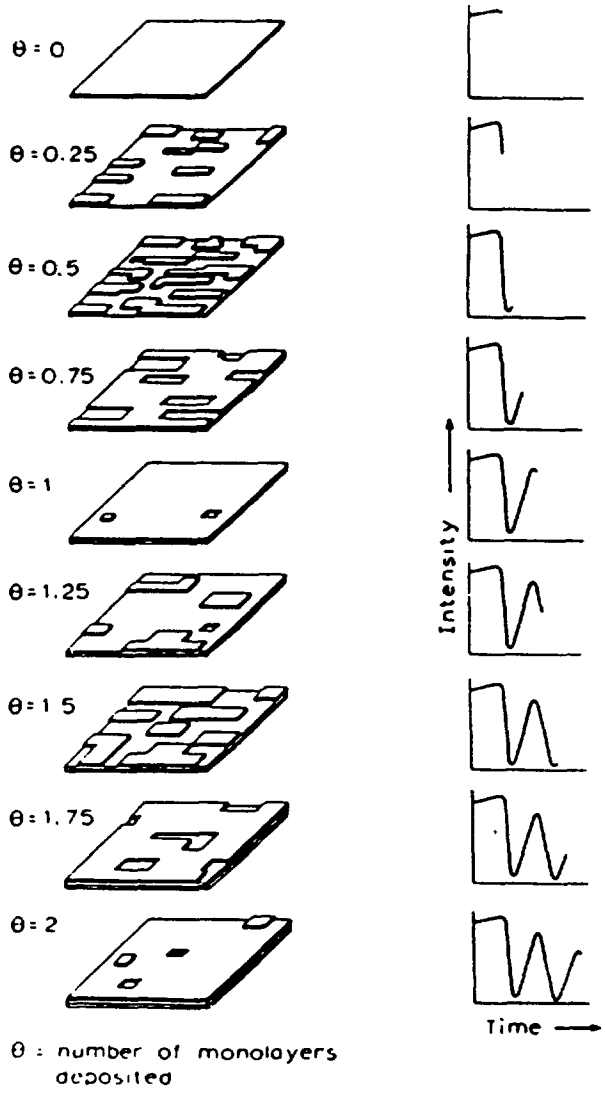

Fig. 6. — Schematic explanation of the evolution of the intensity of the RHEED specular beam with deposition time (on the right). On the left, the different coverages from 0 to 2 ML are represented : the oscillation period is the time taken to grow a single monolayer (from Ref. [23]).

the layer by layer growth. However, it is sometimes difficult to distinguish between the Volmer-Weber and the Stranski-Krastanov modes.

This method has been applied for example to the growth of Pd on reduced Al_2O_3 (0001) and ($1\bar{1}02$) [20] and Cu on stoichiometric TiO_2 (110) [21] : in both cases a Stranski-Krastanov mode was evidenced.

The same formalism can be used to describe the evolution of the photoelectron line intensities measured in an XPS experiment : as an example, a Stranski-Krastanov growth was also observed for Cu on MgO [22].

Another well-suited method for studying the growth mode is the Reflection High Energy Electron Diffraction (RHEED), which is an essential surface science tool for routine MBE.

MBE is used to grow metals, semiconductors and ceramics and is a very general method of crystal growth with particular application where extreme purity and precision are required.

In RHEED experiments, an electron beam, of energy 5 to 30 keV, strikes a single crystal held in the centre of an ultra-high-vacuum chamber with a grazing incidence. The electrons diffracted around the specular direction (glancing detection) fall on a phosphor screen on the other side of the chamber, giving a typically streaked pattern, if the single crystal surface is perfectly flat [23]. Due to the geometry of the experiment, RHEED can be performed *in situ*, during the evaporation, and the evolution of the surface structure can be followed during the growth, while the interface is being formed. Growths which give RHEED streaks, not spots, have a two-dimensional nucleation and growth behaviour, the adatoms remaining in the same plane. On the contrary, three-dimensional growth involves adatoms jumping on top of islands and forming three-dimensional crystals which give rise to RHEED spots, as in transmission experiments.

In the case of a layer by layer growth, the variation of the intensity I of the specular beam with deposition time displays oscillations, the period of the oscillations being equal to the time taken to grow a single monolayer of material. A schematic explanation is given in figure 6. Since the layer thickness is much larger than the de Broglie wavelength of the electrons, the electrons are easily scattered out of the specular beam by the step edges. The step edge concentration is minimum for a complete layer (I maximum) and maximum for 0.5 monolayer coverage (I minimum), hence the oscillations. The damping of the oscillations is due to the increase in the concentration of steps with growth, tending to a limiting equilibrium value.

The RHEED oscillations are routinely used to calibrate the two-dimensional MBE growth of III-V semiconductors. However, to our knowledge, no such studies are yet reported in the literature for the growth of metals on ceramics, likely because the two-dimensional growths for these systems are very scarce. RHEED can nevertheless be useful to get information on the interface structure, as shown in the following section.

3. Atomic structure at the interface.

The atomic structure of the interface can be envisioned from the point of view of the long range order or short range order.

3.1 LONG RANGE ORDER. — As concerns the long range order, electron diffraction techniques like LEED (Low Energy Electron Diffraction) and RHEED can provide useful information on the structure of the interface, when the thickness of the metal deposit is smaller than the probed depth. LEED has been widely used in the past to study surface structures, more precisely surface reconstructions. A new interest is now developing on monocrystalline oxide surface structure, because of their potential use as substrates to grow perfect metal monocrystals on it.

As an example, reconstructions have been observed using LEED and RHEED on a wide range of oxide monocrystalline surfaces, such as: Al_2O_3 $(10\bar{1}2)$ [18], $(11\bar{2}0)$ [24], (0001) [25], MgO (111) [26], Fe_2O_3 (0001) and $(10\bar{1}2)$ [27], TiO_2 (110) [21] and SiO_2 (110) [28].

The interfacial structure obtained by deposing Ni on a monocrystalline Al_2O_3 (0001) (1×1) surface at 800 °C, with an oxygen partial pressure $P_{O_2} = 5 \times 10^{-7}$ Torr, was studied by combining LEED and RHEED [29]. The formation of a $NiAl_2O_4$ spinel phase was shown, in good agreement with the XPS measurements (cf. Sect. 4).

In the case of islanding, it is difficult to obtain information from LEED, the pattern of the bare surface progressively vanishes, due to the attenuation of the diffracted beams across the deposit [30]. In the case of epitaxy, the pattern of the bare surface is progressively replaced by

that of the metal thin film : for instance, the growth of an ultrathin Cu film on room temperature (1 × 1) surfaces of TiO_2 (110) has been studied for coverages ranging from 0 to 80 Å of deposited copper [21]. With increasing deposition thicknesses d_{Cu} up to 7 Å, the diffraction spots of the rectangular substrate pattern were gradually attenuated and the background was relatively increased. No visible extra spots were observed during the initial Cu deposition. A weak hexagonal diffraction pattern, consistent with a slightly contracted Cu (111) film, gradually appeared near d_{Cu} = 7 Å Cu (about 2 monolayers). Subsequent Cu deposition caused further attenuation of the substrate integral spots (completely attenuated for d_{Cu} above 50 Å) and the hexagonal diffraction spots became intense.

3.2 SHORT RANGE ORDER. — As concerns the short range order (local order) one important question is the nature of the adsorption sites at the very beginning of the growth. The methods probing the local order around a given atom, such as SEELFS (Surface Electron Energy Loss Fine Structure Spectroscopy) of SEXAFS (Surface Extended X-ray Absorption Fine Structure Spectroscopy) can be successfully used.

The second method relies on a trustful theoretical background, but requires an incident photon beam with varying energy, so that synchrotron radiation is required. The first method presents the advantage to be possibly carried out in a conventional surface science apparatus, equipped with an electron gun and an electron analyser allowing detection of the electron distribution derivative (Cylindrical Mirror Analyser). The electron energy loss spectrum presents, for energy losses immediately above an ionisation edge, oscillations, which are due to interferences between the wave associated with the emitted electron and the reflected waves from the neighbouring atoms. The EXAFS formalism can be successfully applied to these oscillations, although this has not been rigourously theoretically justified until now, and information on the local structure around the probed atom can be obtained.

The early stages of the growth of Pd clusters on an UHV-cleaved MgO (100) single crystal were investigated by SEELFS [31]. By comparing the ionization peaks corresponding to the oxygen and magnesium K edges on bare MgO with those obtained on MgO covered with Pd clusters of 20 Å diameter, the position of the Pd atoms on the MgO surface could be obtained : the Pd atoms at the interface are on top of the Mg cations.

Due to their sensitivity to the local order around the probed atom, X-ray absorption measurements at a characteristic edge of the deposited atom may bring important information on the local order around the deposited atoms in the initial stages of the deposition, and fruitfully complete other experimental investigations aimed at determining the growth mode, such as Auger Electron Spectroscopy (AES) or X-ray photoelectron spectroscopy (XPS).

As concerns the Cu/Al_2O_3 system, the growth mode was studied by AES and XPS [32-34]. The more recent published work on this topic, carried out on a monocrystalline (0001) (1 × 1) α-Al_2O_3 surface is that of reference [33] : from the evolution of the characteristic Auger signals from substrate and deposit, the authors concluded to a Stranski-Krastanov growth, with one Cu monolayer followed by the formation of clusters. On the other hand, in a previous work [32], performed with an oxidized aluminium substrate, a Volmer-Weber growth mode was evidenced.

Then, X-ray absorption spectroscopy at the CuK edge was used to investigate the first stages of Cu cluster formation when depositing less than one Cu monolayer onto a monocrystalline (0001) stoichiometric α-Al_2O_3 surface [35]. Figures 7 shows the X-ray absorption spectra, in the range 0-50 eV above the threshold, for respectively : a copper reference sample, and 30 % (60 %) Cu monolayer (ML) on stoichiometric α-Al_2O_3 (0001). The 30 % Cu ML spectrum was recorded using CuK_α fluorescence yield detection, as charging effects under the photon beam impeded the use of the total yield detection. For the 60 % Cu ML deposit, these effects

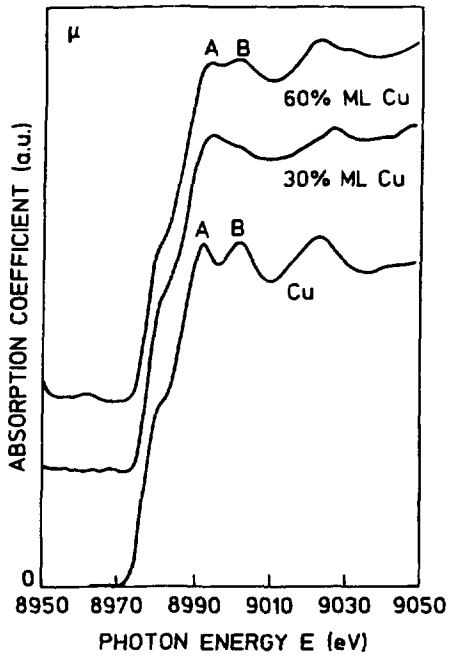

Fig. 7. — CuK absorption edge (XANES spectrum) obtained for respectively : metallic copper (total electron yield detection), 30 % copper monolayer on stoichiometric Al_2O_3 (0001) (CuKα fluorescence yield detection), 60 % copper monolayer on stoichiometric Al_2O_3 (0001) (total electron yield detection) (from Ref. [35]).

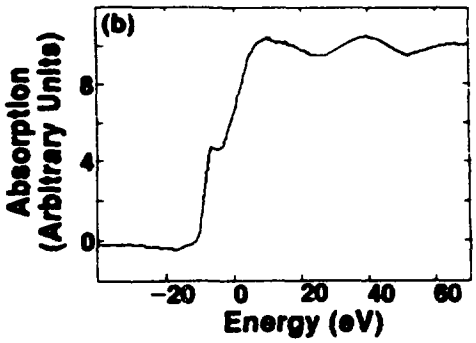

Fig. 8. — CuK absorption edge (XANES spectrum) obtained for 10 Å mean-diameter Cu particles embedded in a solid argon matrix (from [36]).

were weaker and the total electron yield could be measured as a function of photon energy. The XANES spectrum of the 30 % deposit resembles closely that reported in reference [36] (Fig. 8) for clusters with a mean diameter smaller than 15 Å. The XANES spectrum of the 60 % Cu ML deposit is closer to that of metallic copper, with the two characteristic structures A and B well-defined. These structures were shown to arise from multiple scattering involving the fourth- and higher- shell contributions and are smoothed in the small clusters [36].

These results show that even for coverages lower than 1 Cu ML, tridimensional clusters are already formed, indicating a Volmer-Weber growth, in agreement with the conclusion of reference [32]. This was confirmed by the processing of the EXAFS oscillations : the contribution of the first neighbour shell to the EXAFS spectrum could be fitted by using only Cu atoms, at a mean distance 2.49 Å for the 30 % Cu ML deposit. This Cu-Cu distance is characteristic of Cu clusters with a mean diameter smaller than 10 Å [35].

Additional information on the local structure around Cu, as a function of the Al_2O_3 surface structure could be obtained from XPS measurements [30]. The (0001) α-Al_2O_3 surface exhibits after heating at 1 000 °C under UHV a fair (1 × 1) LEED pattern, with a symmetry characteristic of an ideal termination of the bulk. After heating at 1 400 °C under UHV, a more complex diffraction pattern is obtained, identified as $(\sqrt{31} \times \sqrt{31})R \pm 9°$. This reconstruction corresponds to an Al rich surface [25]. The initial stages of the Cu/Al_2O_3 interface formation were investigated by measuring the evolution of the Cu Auger parameter on respectively the (1 × 1) and the $(\sqrt{31} \times \sqrt{31})R \pm 9°$ surface, as a function of the intensity of the Cu $2p_{3/2}$ photoelectron line, normalized to the background level (Fig. 9). On the figure, each point corresponds to a new deposit made on a clean alumina surface, which means that the depositions were not cumulative. The experimental procedure is described in detail elsewhere [30].

The Cu Auger parameter is defined by $A_{Cu} = E_{kin}(CuL_{23}M_{45}M_{45}) - E_{kin}(Cu\ 2p_{3/2}) + h\nu$, $h\nu$ being the photon energy, $E_{kin}(CuL_{23}M_{45}M_{45})$ the energy of the Auger transition and $E_{kin}(Cu\ 2p_{3/2})$ the kinetic energy of the Cu $2p_{3/2}$ photoelectron, both defined with respect to the vacuum level of the spectrometer. It has been shown that this parameter can be determined with a very good accuracy (0.1 eV) [37], and can be used to follow small changes in the chemical environment of copper [38]. Indeed, for a given element involved in two different environments, the variation of the Auger parameter ΔA is related to the variation of the extra-atomic relaxation energy following the creation of the core hole. For copper atoms in an infinite solid, the Cu Auger parameter is characteristic for the oxidation state of the copper atoms [30] : characteristic values of A_{Cu} in Cu_2O, Cu metal and CuO are indicated on the left of

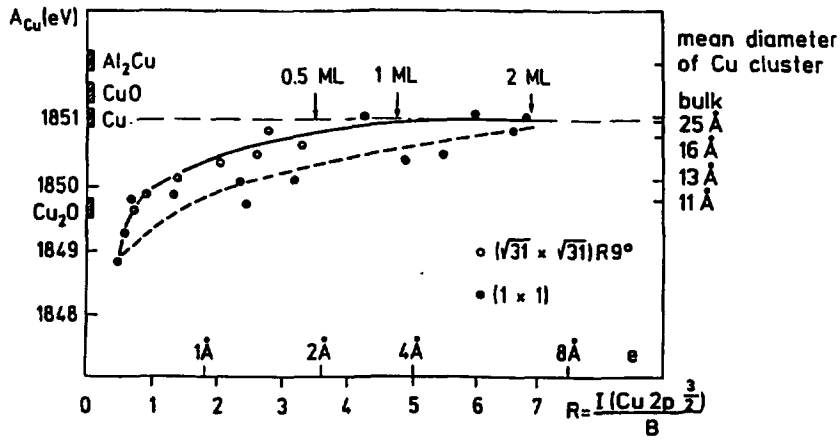

Fig. 9. — Evolution of the copper Auger parameter A_{Cu} as a function of the number of copper atoms at the surface, monitored by the ratio of the intensity of the photoelectron line Cu $2p_{3/2}$ to the background level. The equivalent thicknesses deposited on the quartz microbalance are indicated. On the left side, the characteristic Auger parameters of copper in different compounds are indicated. On the right side, those corresponding to Cu clusters with different sizes.

figure 9. For copper atoms belonging to a cluster, the Auger parameter depends also on the cluster size. On the right of figure 9, A_{Cu} values are indicated as a function of the cluster size, deduced from the work of reference [39], performed on copper clusters supported on a graphite surface.

The evolution of A_{Cu} shows a continuous increase, from Cu(I) to Cu(0) oxidation state. In the initial stages of the growth, copper atoms are chemically bonded to the oxygen atoms of the alumina surface. Then the continuous increase of A_{Cu} is due to the continuous increase of cluster size, until the value characteristic of bulk Cu is achieved.

Assuming in a first approximation that the A_{Cu} variation does not depend on the substrate (this is only an approximation because the polarizability of the substrate will influence the screening of the core hole, hence the A_{Cu} variation), and using the correspondence between A_{Cu} and the cluster size, we observe that, for a given Cu coverage, the cluster size is larger on the reduced reconstructed surface than on the stoichiometric (1 × 1) one. For both surfaces, the growth of copper is of the Volmer-Weber type, but the nucleation is different.

This difference in the nucleation of copper clusters with the reconstruction of the Al_2O_3 (0001) surface has to be compared with the difference we have observed in the thermal stability of thin Cu films evaporated on respectively a (1 × 1) and a $(\sqrt{31} \times \sqrt{31})R \pm 9°$ surface : Cu films with an equivalent 15 Å thickness were deposited onto each surface, kept at room temperature. The deposits were then heated *in situ* under UHV from the room temperature up to 1 300 °C. After each heating, the ratio of the intensities of the Cu $2p_{3/2}$ to the Al 2p photoelectron lines was measured (Fig. 10). The temperature corresponding to a complete desorption of copper, was found to depend on the surface structure : for the (1 × 1) surface, copper was completely desorbed at 1 100 °C, whereas a temperature of 1 300 °C had to be reached on the $(\sqrt{31} \times \sqrt{31})R \pm 9°$ surface.

This result seems to show that the adherence strength of the Cu/Al_2O_3 interface is larger when the Cu film is deposited onto the $(\sqrt{31} \times \sqrt{31})R \pm 9°$ surface than on the (1 × 1) one. This result could reveal a difference in the Cu/Al_2O_3 bonding with the surface reconstruction. Indeed, as shown by the value of the A_{Cu} parameter in the initial stages of the interface formation, and in agreement with previous works [40, 41], Cu bonds to oxygen atoms. But the higher desorption temperature of copper on the aluminium rich $(\sqrt{31} \times \sqrt{31})R \pm 9°$ surface might be due to the formation of an interfacial compound with increasing

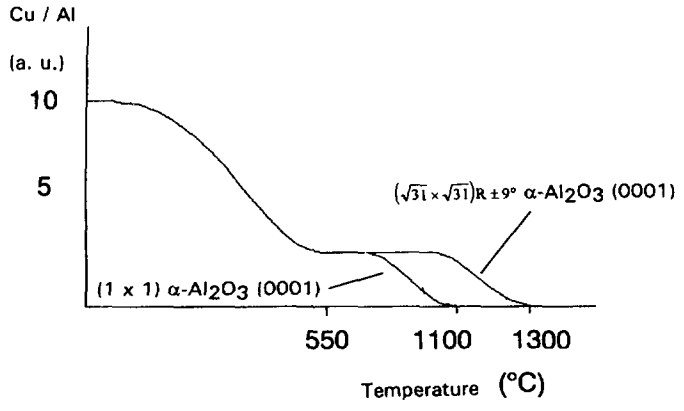

Fig. 10. — Evolution of the ratio of the intensities of the Cu $2p_{3/2}$ and Al 2p photoelectron lines, as a function of temperature, for a 15 Å Cu thin film deposited on respectively a (1 × 1) and a $(\sqrt{31} \times \sqrt{31})R \pm 9°$ a-Al_2O_3 surface (see text).

temperature, with Cu-Al-O bonds. Indeed such bonds, or even formation of a $CuAlO_2$ compound have been observed when the sapphire substrate has been Ar^+ sputtered [42, 43], and then expected to be more Al rich.

Furthermore, the rôle of oxygen in the bond formation between Cu and Al_2O_3 was previously studied [9], using Temperature Programmed Desorption, by varying the deposition conditions : oxygen partial pressure and substrate temperature. The authors showed that the complete desorption of copper was achieved at a larger temperature (about 1 280 °C) when an interfacial $CuAlO_2$ compound has been formed, than when the interface is non reactive (about 1 000 °C-1 100 °C). Comparison between these results and ours seem to strengthen the hypothesis of the formation of Cu-Al-O bonds on the $(\sqrt{31} \times \sqrt{31})R \pm 9°$ α-Al_2O_3 (0001) surface. Work is currently in progress to make this point more precise.

4. Interfacial compounds formation.

The formation of interfacial compounds at the metal-ceramic interface can be studied *in situ*, by varying the deposition conditions, such as the oxygen partial pressure and the substrate temperature. The chemical composition of the interface can be qualitatively obtained by following the shape of a given photoelectron line either from the substrate, or from the deposit [44]. We give herebelow two examples of such studies.

As concerns the Ti/Al_2O_3 interface, the evolution of the Al 2p photoelectron line was studied as a function of Ti coverage, for an Al_2O_3 $(1\bar{1}02)$ surface kept either at room temperature or at 1 000 °C during the Ti evaporation [7]. The appearance of the Al 2p component characteristic of metallic aluminum shows the reduction of the alumina surface by Ti, the higher the substrate temperature and the thicker the deposit, in agreement with the RBS and TEM measurements reported in section 1, which showed the formation of a Ti_3Al interfacial phase.

The $Ni\text{-}Al_2O_3$ interfacial reactions were also studied by a detailed inspection of the Al 2p and Ni 3p photoelectron lines. When Ni was deposited at room temperature under UHV conditions on the cleaned Al_2O_3 (0001) surface, no chemical reaction was detected at the Ni/Al_2O_3 interface. At 800 °C under UHV conditions, a partial reduction of the alumina surface was observed. At 800 °C and with an increased oxygen partial pressure of $P_{O_2} = 5 \times 10^{-9}$ mbar, the shape of the Ni 3p photoelectron line was consistent with the formation of the spinel compound $NiAl_2O_4$ observed by LEED and RHEED, reported in section 3 [29].

5. Summary.

The dynamic processes of the metal-ceramic interface formation can be investigated by condensing a metallic deposit from a vapor phase, onto a monocrystalline ceramic surface prepared *in situ*, the composition, electronic and crystallographic structure of which have been also characterized *in situ*.

The classical surface science methods, relying on the detection of the electrons emitted under an electron or photon beam can then be used, when the interface is being formed. From a number of examples taken in the literature, we have shown how information can be gained on the growth mode, on the local order at the interface (adsorption sites, cluster size...). By varying in a controlled way the substrate temperature and oxygen partial pressure, a detailed study of the interfacial reactions can be obtained, including identification of the interfacial bonds and structure of the interfacial compound.

The progress in the knowledge of the metal-ceramic interfaces requires to complete the experimental surface science approach with thermodynamical models (comparison between the growth mode and the wetting properties, prediction of the interfacial chemical reactions

with substrate temperature and oxygen partial pressure..), and with theoretical modelling of the metal-ceramic electronic structure.

References

[1] McDonald J. E., Eberhart J. G., *Trans. Metall Soc. AIME* **233** (1965) 512-516.
[2] Nicholas M. G., Surfaces and Interfaces of Ceramic Materials, L. C. Dufour Eds. (Kluwer Academic Publishers, 1989) pp. 393-417.
[3] Noguera C., Bordier G., *J. Phys. III France* **4** (1994) 1851.
[4] Epicier T., *J. Phys. III France* **4** (1994) 1811.
[5] Renaud G., *J. Phys III France* **4** (1994) 1795.
[6] Lee C. H., Liang K. S., *Acta Metall Mater.* **40** (1992) S143-S147.
[7] Selverian J. H., Ohuchi F. S., Bortz M., Notis M. R., *J. Mater Sci.* **26** (1991) 6300-6308.
[8] Bourgeois S., Jaumard S., Perdereau M., *Surf. Sci.* **249** (1991) 194-198.
[9] Ohuchi F. S., Metal-Ceramic Interfaces, Acta Scripta Metallurgica Proceedings Series, vol. 4, M. Rühle, A. G. Evans, M. F. Ashby, J. P. Hirth Eds. (Pergamon Press, Elmsford, NY, 1990) pp. 93-106.
[10] Dufour L. C., Perdereau M., Surfaces and Interfaces of Ceramic Materials, L. C. Dufour Ed. (Kluwer Academic Publishers, 1989) pp. 419-448.
[11] Neugebauer C. A., Handbook of thin films technology, Maisel and Glang Eds. (McGraw Hill, 1970) pp. 8.3-8.44.
[12] Henry C. R., Chapon C., Duriez C., Giorgio S., *Surf. Sci.* **253** (1991) 177-189.
[13] Winterbottom W. L., *Acta Met.* **15** (1967) 303-310.
[14] Sood D. K., Baglin J. E. E., *Nucl. Instr. Meth. B* **19/20** (1987) 954-958.
[15] Eustathopoulos N., *J. Phys III France* **4** (1994) 1865.
[16] Guglielmachi J. M., Thesis, Marseille University (1982).
[17] Ernst H. J., Fabre F., Lapujoulade J., *Surf. Sci. Lett.* **275** (1992) L682-L684.
[18] Gillet E., Legressus C., Gillet M., *J. Chim. Phys.* **84** (1987) 167-174.
[19] Feldman L. C., Mayer J. W., Fondamentals of surface and thin film analysis (Elsevier Science Publishers, Amsterdam, the Netherlands, North Holland, 1986) pp. 136-139.
[20] Ricci M., Ealet B., Gillet E., Gillet M., *Le Vide, Les Couches Minces* **260** (1992) 350-352.
[21] Moller P. J., Wu M. C., *Surf. Sci.* **224** (1989) 265-276, and references therein.
[22] Alstrup I., Moller P. J., *Appl. Surf. Sci.* **33/34** (1988) 143-151.
[23] Price G. L., Surface Analysis Methods in Materials Science, D. J. O'Connor, B. A. Sexton, R. St. C. Smart Eds., *Springer Series Surf Sci.* **23** (1992) 263-274.
[24] Hsu T., Kim Y., *Surf. Sci. Lett.* **243** (1991) L63-L66.
[25] Gautier M., Duraud J. P., Pham Van L., Guittet M. J., *Surf Sci.* **250** (1991) 71-80, and references therein.
[26] Gajdardziska-Josifovska M., Crozier P. A., Cowley J. M., *Surf Sci. Lett.* **24** (1991) L259-L264.
[27] Lad R. J., Henrich V. E., *Surf. Sci* **193** (1988) 81-93.
[28] Bart F., Gautier M., Duraud J. P., Henriot M., *Surf. Sci* **274** (1992) 317-328.
[29] Zhong Q., Ohuchi F. S., *J. Vac. Sci. Technol. A* **8** (1990) 2107-2112.
[30] Gautier M., Duraud J. P., Pham Van L., *Surf. Sci Lett.* **249** (1991) L327-L332.
[31] Goyhenex C., Henry C. R., *J Electron Spectrosc. Relat Phenom.* **61** (1992) 65-83.
[32] Di Castro V., Polzonetti G., *Surf. Sci* **189/190** (1987) 1085-1090.
[33] Moller P. J., Guo Q., *Thin Solid Films* **201** (1991) 267-279.
[34] Chen J. G., Colaianni M. L., Weinberg W. H., Yates J. T., *Surf Sci* **279** (1992) 223-232.
[35] Gautier M., Pham Van L., Duraud J. P., *Europhys Lett.* **18** (2) 1992, 175-180.
[36] Montano P. A., Shenoy G. K., Alp E. E., *Phys. Rev. Lett* **43** (1986) 2076-2079.
[37] Waddington S. D., Weightman O., Mathew J. A. D., Grassie A. D. M., *Phys. Rev. B* **39** (1989) 10239-245.

[38] Wagner C. D., *J. Electron Spectros. Relat. Phenom.* **10** (1977) 305-315.
[39] de Crescenzi M., Diociaiuti M., Lozzi L., Picozzi P., Santucci S., Battistoni C., Mattogno G., *Surf. Sci.* **178** (1986) 282-289.
[40] Kasowski R. V., Ohuchi F. S., French R. H., *Physica B* **150** (1988) 44-46.
[41] Guo Q., Moller P. J., *Surf. Sci.* **244** (1991) 228-236.
[42] Baglin J. E. E., Schott A. G., Thompson R. D., Tu K. N., Segmüller A., *Nucl. Instrum. Methods B* **19/20** (1987) 782-786.
[43] Schott A. G., Thompson R. D., Tu K. N., *Mater. Res. Soc. Symp. Proc.* **60** (1986) 331-336.
[44] Ohuchi F. S., Kohyama M., *J. Am. Ceram. Soc.* **74** (1991) 1163-1187.